

Contactless electroreflectance of CdSe/ZnSe quantum dots grown by molecular-beam epitaxy

Martín Muñoz,^{a)} Shiping Guo, Xuecong Zhou, and Maria C. Tamargo

Chemistry Department, City College of the City University of New York, Convent Avenue at 138th Street, New York, New York 10031

Y. S. Huang

Department of Electronic Engineering, National Taiwan University of Science and Technology, Taipei 106, Taiwan, Republic of China.

C. Trallero-Giner and A. H. Rodríguez

Departamento de Física Teórica, Facultad de Física, Universidad de La Habana San Lazaro y L, 10400 La Habana, Cuba

(Received 9 June 2003; accepted 23 September 2003)

The interband transitions of a capped CdSe quantum-dot structure have been investigated using contactless electroreflectance. The electroreflectance spectrum shows transitions originating from all the portions of the sample including the quantum dots and the wetting layer. The transitions of the two-dimensional layers have been modeled using an envelope approximation calculation which takes into account the biaxial strain in the wetting layer. A good agreement was found between the experimental values for the transition energies and the calculated ones. From atomic force microscopy measurements, a lens shape was observed for the uncapped quantum dots. Taking into account the lens shape geometry and assuming that the effective height-to-radius ratio is preserved, the size of the capped quantum dots was determined using the observed electroreflectance transitions, in the framework of the effective mass approximation. © 2003 American Institute of Physics. [DOI: 10.1063/1.1628393]

In recent years there have been increasing efforts in the development of quantum dot (QD) semiconductor nanostructures. Technological applications anticipated for these structures motivate this trend. Among them is their stimulated emission,^{1,2} which exhibit excellent lasing characteristics in agreement with theoretical predictions,³ making the QD structures a potential candidate to replace the quantum well lasers.¹ Self-assembled (SA) QDs grown using the Stranski–Krastanov growth mode are the subject of intensive study.^{2,4} Most of the studies of SA QDs have been performed in III–V semiconductor systems such as InGaAs/GaAs,⁵ InP/InGaP,⁶ and GaSb/GaAs.⁷ Much less has been done in the II–VI systems, which are potentially attractive for applications in visible wavelength range. The optical properties of SA QDs have been widely studied using photoluminescence (PL),^{1,2,8,9} photoluminescence excitation spectroscopy,^{8,9} and time resolved photoluminescence,¹⁰ however, the information obtained is restricted to lower energy states and does not allow to study the shape of the QD potential or the coupling effects in stacked structures. Even though modulation spectroscopy allows one to perform studies of the lower as well as the higher energy transitions in QD structures very little work has been done on this subject.¹¹ In this letter we present a contactless electroreflectance (CER) study of CdSe QDs with ZnSe barriers.

Two samples were prepared by molecular-beam epitaxy (MBE) using a dual chamber Riber 2300P MBE system that includes a chamber for the growth of As-based III–V materials and another for the growth of wide band gap II–VI

compounds. The two chambers are connected by ultrahigh vacuum transfer modules. Semi-insulating epitaxially grown GaAs (100) substrates were mounted on 2 in. molybdenum blocks and introduced in the MBE system where they were deoxidized in the III–V chamber under an As flux. In order to have a flat surface for the QD formation a 200 nm GaAs buffer layer followed by a 30 period (19 Å GaAs/20 Å AlAs) short-period superlattice (SL) and a 30 nm GaAs layer were grown at 580 °C. These buffer layers were grown under As-rich conditions having a (2×4) surface reconstruction. The use of the SL produces very smooth surfaces.¹² Then the substrates were transferred to the II–VI chamber. Prior to the growth of the II–VI materials, the surface of each substrate was exposed to a Be–Zn flux (Zn–Be irradiation) for 40 s at 170 °C. This step avoids the formation of stacking faults at the II–VI/III–V interface.¹³ Then on each sample a ZnSe buffer layer (6 nm) was grown at 250 °C followed by 94 nm of ZnSe at 270 °C. The CdSe QDs were formed by depositing 2.5 MLs of CdSe on ZnSe at 320 °C, after a growth interruption of 30 s, in the case of the sample used for PL and CER measurements, a ZnSe top barrier or cap layer of 100 nm was grown at 270 °C to confine the QDs. No cap layer was grown on the sample used for atomic force microscopy (AFM) measurements. The capped QD structure was characterized by PL measurements using the 325 nm line of a HeCd laser for excitation. The QD PL peak was detected at 2.372 and 2.319 eV at 77 and 300 K, respectively, no deep-level emission was observed.

The interband transitions in this structure were determined using CER,¹⁴ which is a modulated technique,^{15,16} that gives rise to sharp, differential-like spectra in the region of

^{a)}Author to whom correspondence should be addressed; electronic mail: mmunoz@sci.ccnycuny.edu

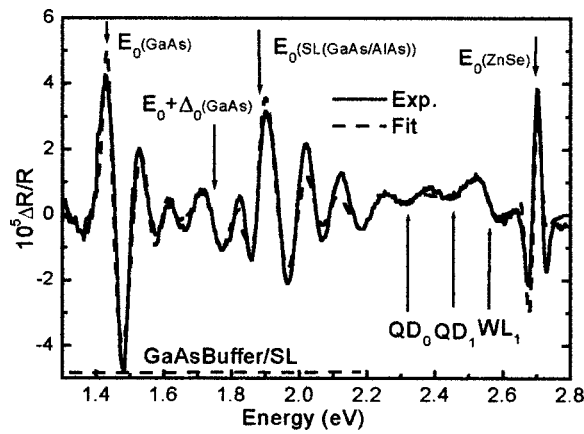


FIG. 1. CER spectrum of capped CdSe quantum dot structure. Solid and dashed lines represent the experimental data and fit, respectively. The arrows indicate the energies obtained from our fit scheme.

the transitions. The experimental details and principles of CER are explained in Ref. 14.

The AFM studies were performed immediately after the samples were grown. From the AFM images we found that the dots have a lens shape with average radius of $r=52.5$ nm, an average height of $h=18$ nm, an effective ratio $h/r=0.34$ and a dot density of $4.6 \times 10^8 \text{ cm}^{-2}$.

The solid line in Fig. 1 is the measured RT CER spectrum. The energies corresponding to the observed transitions were obtained using a fit, shown by the dashed line. The transitions originating in the SL/buffer region (<2.2 eV) present a series of Franz–Keldysh oscillations, and were fit using Lorentzian broadened electro-optical functions.¹⁴ The transitions originating from the QDs, wetting layer (WL), and barrier (>2.2 eV) were fit using the first derivative of a Gaussian line shape¹⁴ due to their bound origin. The values obtained from this fit are indicated by arrows in the figure and presented in Table I.

The identification of the signals coming from the GaAs buffer layer at $E_0(\text{GaAs})$, $E_0 + \Delta_0(\text{GaAs})$, and ZnSe barriers at $E_0(\text{ZnSe})$, respectively, were straightforward when compared with the established values in the literature, as shown in Table I. The assignment of the other transitions was done according to the following considerations. Using a three-band model envelope calculation,¹⁷ a band offset parameter $Q_c = \Delta E_c / \Delta E_g = 0.65$, $E_0(\text{GaAs}) = 1.428$ eV and the effective masses and spin-orbit splitting of GaAs and AlAs given in Ref. 18 we obtained that the lowest transition, $1C-1H$, for this short period SL is 1.876 eV, which agrees well with the signal at 1.873 eV. The notation $mC-nH(L)$ refers to the transition between the m th conduction and the n th valence state of heavy or light hole character, respectively. In order to identify the transition coming from the WL we performed an envelope calculation¹⁷ taking into consideration that the biaxial strain changes the CdSe band gaps. Reference 19 describes the changes in the band gaps as a function of the elastic constants C_{11} , C_{12} and deformation potentials a and b , which were obtained from Refs. 19–21 for this calculation. We have considered that the conduction band offset is described by the parameter $Q_c = 0.85$.²² The parameters required for this calculation are presented in Table II. Assuming that there is no intermixing between the WL and the ZnSe barriers the WL lowest heavy hole transition, $1C-1H$,

TABLE I. Experimental and calculated interband transition energies.

Transition	Experiment (eV) (± 0.005)	Theory (eV)	PL (eV) (± 0.002)
$E_0(\text{GaAs})$	1.428 (1.422 ¹⁸)		
$E_0 + \Delta_0(\text{GaAs})$	1.745 (1.762 ^a)		
SL(GaAs/AlAs)	1.873	1.876	
$1C-1H$			
QD_0	2.320	2.320	2.319
$ 1,0\rangle_e \rightarrow 1,0\rangle_{hh}$			
QD_1	2.455	2.455	
$ 1,1\rangle_e \rightarrow 1,1\rangle_{hh}$			
WL_1	2.560	2.560 ^b	
$1C-1H$			
$E_0(\text{ZnSe})$	2.700	2.700 ³⁰	

^a E_0 and Δ_0 were obtained from Refs. 18 and 20, respectively.

^b4.7 Å (~ 1.5 ML) CdSe wetting layer.

and thickness are 2.560 eV and 4.7 Å ≈ 1.5 ML, respectively. In order to identify the transitions originating from the QDs, the shape of the quantum lens has been modeled by a spherical cap of height h and circular cross section with radius r . For the sake of simplicity and in the limit of strong spatial confinement regime, we have applied our calculation here to the uncoupled electron-hole particle Hamiltonian model confined in the QD domain with isotropic bands and effective masses m_e and m_h for the electron and holes, respectively. It is possible to show²³ that the electron-hole pair energy $E_{N_e M_e; N_h M_h}$ depends on the aspect ratio h/r , the electron and hole energy levels, N_e and N_h , and the z-component of the angular orbital momentum associated to the electron and hole, M_e and M_h , respectively. According to the allowed optical selection rules, the features observed in the CdSe QD spectral region correspond to the transitions $|N, M\rangle_e \rightarrow |N, M\rangle_h$. As we mentioned, the ratio h/r for our lens-shaped quantum dots is 0.34. Assuming that this ratio minimizes the energy surface in this system and, therefore, is the most favorable ratio for QDs formation, and using the effective masses given in Table II, we determined that the dimensions of the capped CdSe–QDs corresponding to these QD_0 and QD_1 transitions are $h=3.24$ nm and $r=9.52$ nm. According to this calculation the features QD_0 and QD_1 corre-

TABLE II. Values of the parameters used in the calculation.

Parameter	ZnSe	CdSe
E_0 (eV), 300 K	2.700 ^a	1.692 ²⁹
m_e	0.15 ^b (0.13...0.17)	0.11 ³⁰
m_{hh}	0.66 ^b (0.57...0.75)	0.44 ³⁰
Δ_0 (eV)	0.43 ³¹	0.42 ³¹
C_{11}	8.5 ^c	6.67 ^c
(10^{11} dyn/cm ²)		
C_{12}	5.02 ^c	4.63 ^c
(10^{11} dyn/cm ²)		
a (eV)	−5.4 ^c	−3.0 ^c
b (eV)	−1.2 ^c	−0.7 ^c

^aExperimental value.

^bAverage of the values shown in parentheses, these values were obtained from Ref. 30.

^cReferences 19–21.

spond to the electron→heavy hole transitions $|1,0\rangle_e \rightarrow |1,0\rangle_{hh}$ and $|1,1\rangle_e \rightarrow |1,1\rangle_{hh}$, respectively. From this calculation we observed that the capped QD sizes are approximately five times smaller than the uncapped ones. We suggest that the increased size of the uncapped QDs is largely due to ripening phenomenon (RP). Ripening in the uncapped dots can occur due to the absence of the ZnSe cap layer that allows surface migration. As a result some QDs grow at the expense of others, while the ZnSe cap layer will limit this movement.

This RP has been observed previously in CdSe QDs grown on ZnSe.²⁴ Reference 24 performed a study of the RP by monitoring the uncapped-QD dimensions as a function of time using AFM measurements. Making an extrapolation for the time $t=0$ s after the QDs growth and considering a correction due to the AFM tip size they reported that the diameter of the buried QDs is 35 nm, suggesting that their QDs were bigger than ours. The observation that the QDs of Ref. 24 are bigger than those studied in this work is confirmed by their PL emission of 2.32 eV and full width at half maximum (FWHM)=80 meV, at 10 K, while the PL emission energy of the QDs presented here is 2.372, FWHM=56 meV at 77K. The difference between the QD size presented in Ref. 24 and in this work is due to the fact that the QDs in Ref. 24 were grown using a substrate temperature of 370 °C, while the ones presented here were grown at 320 °C. This observation is in agreement with the scanning tunneling microscopy studies of the dimension of the InAs/GaAs QDs as function of the growth temperature,^{25,26} which concluded that the higher the growth temperature the bigger the QDs. Moreover, this trend was shown analytically for spherical QDs.^{26,27} The WL and QDs dimensions obtained in this study, while assuming no intermixing provide the lower limit of the dimensions of these structures. If some intermixing occurs, the presence of Zn in these structures will blueshift the energies of the transitions if their size remains the same, therefore in order to fit the transition energies an increase in the structure dimensions is necessary. Raman studies on these samples²⁸ show that the WL and QDs longitudinal optical phonon energies correspond to compositions with less than 10% of Zn, supporting the hypothesis of small degree of intermixing made in our modeling.

In summary, we determined the interband transition energies of a CdSe-QD structure using CER. The observed transitions originate from all parts of this structure including the QDs and wetting layer. From the calculation of the energy transitions it was found that the WL feature corresponds to the $1C-1H$ transition while the QD features QD_0 and QD_1 correspond to transitions $|1,0\rangle_e \rightarrow |1,0\rangle_{hh}$ and $|1,1\rangle_e \rightarrow |1,1\rangle_{hh}$. Assuming a lens shape geometry with a height/radius ratio=0.34 is the most energetically favorable configuration for the QD shape in this system, we found that the capped QDs dimensions in our structure are $h=3.24$ nm and $r=9.52$ nm.

This work was supported by the National Science Foundation through Grant No. ECS0217646. Partial support was also obtained from the Center for Analysis of Structures and Interfaces, and the New York State Center for Advanced Technology on Photonic Materials and Applications.

- ¹N. Kirstaedter, O. G. Schmidt, N. N. Ledentsov, D. Bimberg, V. M. Ustinov, A. Yu. Egorov, A. E. Zhukov, M. V. Maximov, P. S. Kop'ev, and Zh. I. Alferov, Appl. Phys. Lett. **69**, 1226 (1996).
- ²N. N. Ledentsov, V. A. Shchukin, M. Grundmann, N. Kirstaedter, J. Böhrer, O. Schmidt, D. Bimberg, V. M. Ustinov, A. Yu. Egorov, A. E. Zhukov, P. S. Kop'ev, S. V. Zaitsev, N. Yu. Gordeev, Zh. I. Alferov, A. I. Borovkov, A. O. Kosogov, S. S. Ruvimov, P. Werner, U. Gösele, and J. Heydenreich, Phys. Rev. B **54**, 8743 (1996).
- ³M. Asada, Y. Miyamoto, and Y. Suematsu, IEEE J. Quantum Electron. **QE-22**, 1915 (1986).
- ⁴S. P. Guo, X. Zhou, O. Maksimov, M. C. Tamargo, C. Chi., A. Couzis, C. Maldarelli, I. L. Kuskovsky, and G. F. Newmark, J. Vac. Sci. Technol. B **19**, 1635 (2001).
- ⁵A. Madhukar, Q. Xie, P. Chen, and A. Konkar, Appl. Phys. Lett. **64**, 2727 (1994).
- ⁶A. Kurtenbach, K. Eberl, and T. Shitara, Appl. Phys. Lett. **66**, 361 (1995).
- ⁷F. Hatami, N. N. Ledentsov, M. Grundmann, J. Böhrer, F. Heinrichsdorff, M. Beer, D. Bimberg, S. S. Ruvimov, P. Werner, U. Gösele, J. Heydenreich, U. Richter, S. V. Ivanov, B. Ya. Mel'tser, P. S. Kop'ev, and Zh. I. Alferov, Appl. Phys. Lett. **67**, 656 (1995).
- ⁸K. H. Schmidt, G. Medeiros-Ribeiro, M. Oestreich, and P. M. Petroff, Phys. Rev. B **54**, 11346 (1996).
- ⁹R. Heitz, M. Grundmann, N. N. Ledentsov, L. Eckey, M. Veit, D. Bimberg, V. M. Ustinov, A. Yu. Egorov, A. E. Zhukov, P. S. Kop'ev, and Zh. I. Alferov, Appl. Phys. Lett. **68**, 361 (1996).
- ¹⁰S. Raymond, S. Fafard, P. J. Poole, A. Wojs, P. Hawrylak, S. Charbonneau, D. Leonard, R. Leon, P. M. Petroff, and J. L. Merz, Phys. Rev. B **54**, 11548 (1996).
- ¹¹F. H. Pollak, in *Nano-Optoelectronics*, edited by M. Grundmann (Springer, Berlin, 2002), pp. 215–238, and references therein.
- ¹²C. Weisbuch and B. Vinter, *Quantum Semiconductor Structures* (Academic, San Diego, 1991), p. 6.
- ¹³D. Li and M. D. Pashley, J. Vac. Sci. Technol. B **12**, 2547 (1994).
- ¹⁴F. H. Pollak, in *Group III Nitride Semiconductor Compounds*, edited by B. Gil (Clarendon, Oxford, 1998), p. 158.
- ¹⁵F. H. Pollak and H. Shen, Mater. Sci. Eng., R. **10**, 275 (1993).
- ¹⁶M. Cardona, *Modulation Spectroscopy* (Academic, New York, 1969).
- ¹⁷G. Bastard and J. A. Brum, IEEE J. Quantum Electron. **QE-22**, 1625 (1986); G. Bastard, *Wave Mechanics Applied to Semiconductor Heterostructures* (Les editions de Physique, Cedex, France, 1988).
- ¹⁸S. H. Pan, H. Shen, Z. Hang, F. H. Pollak, W. Zhuang, Q. Xu, A. P. Roth, R. A. Masut, C. Lacelle, and D. Morris, Phys. Rev. B **38**, 3375 (1988).
- ¹⁹F. H. Pollak, in *Effects of Uniaxial Stress on the Optical Properties of Semiconductors and Semiconductor Microstructures*, Semiconductors and Semimetals Vol. 55, edited by R. K. Willardson and A. C. Beer (Academic, San Diego, 1998), Chap. 4.
- ²⁰Landolt-Börnstein, *Numerical Data and Functional Relationships in Science and Technology*, edited by O. Madelung, M. Schultz, and H. Weiss (Springer, New York, 1982), Vol. III/11.
- ²¹A. Blacha, H. Presting, and M. Cardona, Phys. Status Solidi B **126**, 11 (1984).
- ²²T. P. Surkova, M. Godlewski, K. Swiatek, P. Kaczor, A. Polimeni, L. Eaves, and W. Giriat, Physica B **273–274**, 848 (1999).
- ²³A. H. Rodríguez, C. Trallero-Giner, S. E. Ulloa, and J. Marín-Antuña, Phys. Rev. B **63**, 125319 (2001); A. H. Rodríguez, Carlos R. Handy, and C. Trallero-Giner, J. Phys. A (to be published).
- ²⁴J. L. Merz, S. Lee, and J. K. Furdyna, J. Cryst. Growth **184–185**, 228 (1998).
- ²⁵O. Suekane, S. Hasegawa, T. Okui, M. Takata, and H. Nakashima, Jpn. J. Appl. Phys., Part 1 **41**, 1022 (2002).
- ²⁶O. Suekane, in *Nano-Optoelectronics*, edited by M. Grundmann (Springer, New York, 2001).
- ²⁷I. V. Markov, *Crystal Growth for Beginners* (World Scientific, Singapore, 1995).
- ²⁸Y. Gu and I. L. Kuskovsky (private communication).
- ²⁹R. E. Nahory, M. J. S. P. Brasil, and M. C. Tamargo, in *Semiconductor Interfaces and Microstructures*, edited by Z. Feng (World Scientific, Singapore, 1992), p. 238.
- ³⁰*Semiconductors—Basic Data*, 2nd ed., edited by O. Madelung (Springer, Berlin, 1996).
- ³¹P. Lawaetz, Phys. Rev. B **4**, 3460 (1971).